

Copyright © IFAC Computer Applications in Biotechnology,
Québec City, Canada, 2001

CHARACTERISATION OF ACTIVATED SLUDGE BY AUTOMATED IMAGE ANALYSIS : VALIDATION ON FULL-SCALE PLANTS

M. da Motta*, **L.P. Amaral******, **M. Casellas*****, **M.N. Pons***, **C. Dagot*****,
N. Roche**, **E.C. Ferreira******, **H. Vivier****

**Laboratoire des Sciences du Génie Chimique, CNRS-ENSIC-INPL, Nancy, France*

***IUT de Marseille, Univ. Marseille, France*

****ENSIL, Limoges, France*

*****Centro de Engenharia Biológica-IBQF, Univ. do Minho, Braga, Portugal*
Marie-Noelle.Pons@ensic.inpl-nancy.fr

Abstract : Automated methods based on the analysis of macro- and meso-scale images has been developed to characterise activated sludge in terms of size and shape (fractal dimension) of flocs and abundance of filamentous bacteria. After tests on pilot-scale reactors, the method has been validated on full-scale samples from twelve different wastewater treatment plants in France and Portugal. *Copyright 2001 IFAC*

Keywords : Activated sludge, flocs, morphology, filamentous bacteria, image analysis

I. INTRODUCTION

The biological reactor of a wastewater treatment plant by activated sludge is a complex ecosystem, composed of different types of bacteria, protozoa and metazoa, in charge of the degradation of the pollution. Zooglyphic bacteria are agglomerated as flocs, owing to exopolymers they excrete and to filamentous bacteria which constitute the floc backbone. A good balance between the different types of bacteria is essential to good settleability properties in the final clarifier and a good quality of the effluent. In absence of filamentous bacteria, small flocs are observed, that do not settle correctly ("pinpoint" bulking). When the filamentous bacteria are in excess, the flocs do not settle correctly either ("filamentous bulking"). This over-development is generally due to substrate limitation or excess. There are different types of filamentous bacteria: *Microthrix parvicella* are found generally in Europe (Eikelboom, *et al.*, 1998; Wanner, *et al.*, 1998; Westlund, *et al.*, 1996) when *Nocardia* sp. and Type 1701 are prevailing in the US (Richard, 1991).

The classical method to characterise the flocs and evaluate the amount of filamentous bacteria is to count them under a microscope. It is a tedious and rather imprecise method. Some authors have tested automated image analysis methods to characterise the floc morphology, mainly in terms of their fractal dimension, and to relate it to settleability properties (Grijpsperdt and Verstraete, 1996, 1997).

Automated image analysis seems indeed a good method to characterise quantitatively both flocs and filamentous bacteria. A reliable information of this type should enable to improve the daily operation of wastewater treatment plants. Such a method has been proposed by da Motta *et al.* (1999, 2000a) and used to monitor bulking events in pilot plants (Alves *et al.*, 2000; da Motta *et al.*, 2000b). The results of validation trials on full-scale wastewater treatment plants are here discussed.

II. MATERIALS AND METHODS

2.1. Sampling

Mixed liquor samples were taken in 12 full-scale plants of different size, design and locations (7 in Lorraine (F), 2 in Limousin (F) and 3 in Minho (P)).

2.2. Image capture

Optical microscopes equipped with a video camera and connected to a PC via a grabbing board were used in the three locations. A drop of fresh mixed liquor was carefully deposited on a glass slide and covered with a cover slip. The slide was immediately observed. Series of 70 images (meso-scale visualisation at magnification $\times 100$, bright field illumination) and, for some samples, of 50 images (macro-scale visualisation at magnification $\times 25$, black field illumination) were grabbed by a systematic examination of the slide. The 756x576 pixels or 512x341 pixels 8bits-images were analysed using procedures embedded within Visilog™ (Noésis, les Ulis, France).

2.3. Physico-chemical analysis

The sludge concentration (C_0) was measured by centrifugation of a sample aliquot for 15 min at 3000 and by drying the solid residue for 12 hours at 105°C. After weighting, the residue was placed in an oven at 550°C for the determination of the volatile suspended solids (VSS). The percentage of volatile suspended solids is defined as:

$$\%VSS = 100 \cdot VSS / C_0 \quad (1)$$

The settleability characteristics were measured in a cylindrical column. The sludge height variation versus time, $h(t)$, was monitored for 30 min at least. The data were analysed according to Kynch's theory (1952). The average settling velocity (v_s) is calculated by linear regression in the free-falling zone. The Sludge Volume Index (SVI) (L/g) is defined as:

$$SVI = \frac{H_{30}}{H_0 C_0} \quad (2)$$

where H_0 and H_{30} are respectively the height of the sludge at time = 0 and time = 30 min. In some cases, due to bad settleability properties, it was necessary to dilute the sludge to run the test.

2.4. Meso-scale image analysis

The grey-level images are initially enhanced (histogram equalisation, delineation, halo suppression by subtraction of a background image obtained after applying a 55-iteration opening to the initial grey-level image). The resulting image is then

automatically segmented: the segmentation algorithm considers the variance of the grey-level histogram. On the resulting binary image, the discrimination between flocs on one hand and small debris and filaments on the other hand is based on their size difference. To separate the filaments from small debris a size and morphological filter, based on the reduced gyration radius, is applied.

Figure 1 presents some typical grey-level images with the corresponding flocs and filaments binary images. The filamentous bacteria should be characterised by their total length and by their number to discriminate between short and long filaments. Although it has not been checked, the bacteria of Figure 1a and 1b are probably of different species. The activated sludge pictured in Figure 1 contains 13% (1a) and 64% (1b) of filamentous bacteria, as calculated in terms of projected area.

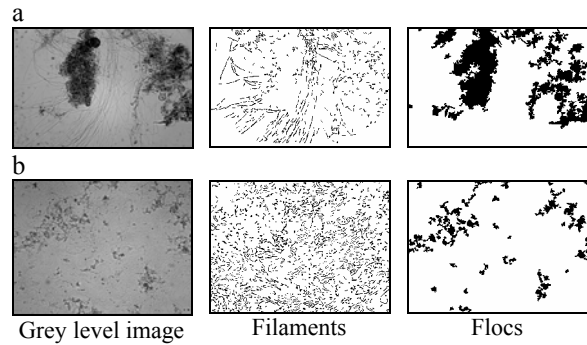


Fig. 1: Examples of image analysis final results

The filaments are characterised by their number (N_f) and the total length of their skeleton (L_f) per image. The flocs are characterised by their projected surface (S) and fractal dimension (D_f). The fractal dimension is calculated according to the method proposed by Russ (1995) and based on the Euclidian Distance map. The equivalent diameter in surface, D_{eq} , is deduced from S :

$$D_{eq} = 2\sqrt{S/\pi} \quad (3)$$

2.5 Macro-scale image analysis

The 100x magnification is well adapted to the characterisation of filaments but it appears on some samples that the floc size might be under-estimated, because many flocs are cut by the frame edges. A lower magnification, with black-field illumination has then been tested. Figure 2 presents some images obtained in these conditions. The initial and final steps of the treatment (halo suppression, segmentation, debris removal) are presented in Figure 3. It appears however that the size measurement based on the equivalent diameter in surface as defined in Eq. 3 might be inadequate, as large and very complex floc areas are visible, due to high suspended solids concentration. Therefore the

size distribution was also assessed by series of hexagonal openings. The average size D_h is the size of the average hexagon which can be inscribed in the flocs (Russ, 1995).

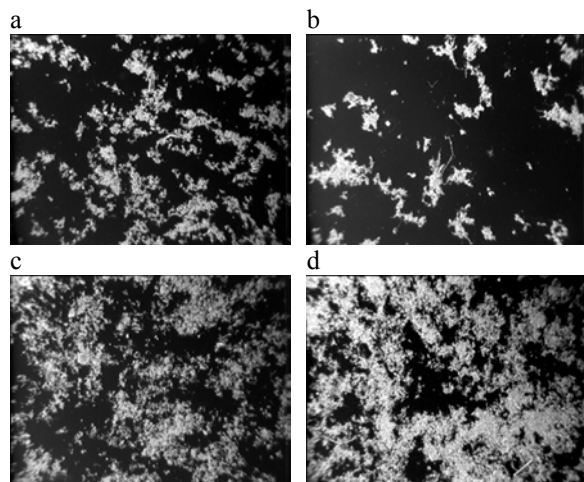


Fig.2. Typical black-field images for samples 3 (a), 4 (b), 10 (c) and 12 (d)

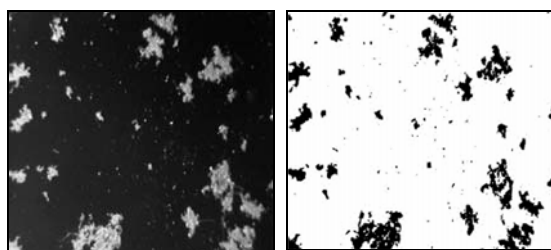


Fig. 3. Initial grey-level image and final binary image

III. RESULTS

3.1 Physico-chemical characterisation

The results of the physico-chemical analyses are given in Table 1 and 2. The high suspended solid concentration and low %VSS observed in sample 3 are related to a chemical precipitation of phosphorus. When SVI could not be correctly measured ($H_{30}/H_0 > 0.5$) the mixed liquor sample was diluted with plant effluent water. For sample 9, it was not possible to obtain any visible settlement without dilution.

It is difficult to compare the settleability properties of the samples based on SVI due to the dilution factor which had to be applied to have a reasonable decrease of the sludge height in the test column. Nevertheless, it appears that most samples have rather bad settleability characteristics.

3.2 Meso-scale morphology

Table 3 summarises the main results obtained by image analysis. The values correspond to the averages calculated on 70 images per sample.

There is a general agreement between the abundance given by image analysis and the visual examination

of the images. Some discrepancies were however noticed and analysed. In sample 7, flocs could appear with very low or very high grey-level. This problem was not expected initially in the image treatment and some flocs were mistaken as filaments. For samples 8 and 9, the visualisation system had a lower spatial resolution than for the other samples. It was necessary to adapt some image analysis parameters. However very thin filaments attached to flocs in sample 8 could not be detected properly.

Table 1: SS and %VSS of the full-scale plant samples

Sample	SS (g/L)	%VSS
1	3.8	65
2	4.8	64
3	10.4	60
4	1.7	75
5	2.5	85
6	2.8	76
7	3.2	73
8	4.6	n.a.
9	7.2	n.a.
10	5.0	69
11	3.1	64
12	9.5	69

Table 2: Settleability characteristics. n.a. = non available; dil = diluted; * dilution factor 1:2

Sample	SVI (L/g)	H_{30}/H_0	dil. factor	SVI dil (L/g)	H_{30}/H_0 dil	V_0 (cm/min)
1	0.238	0.91	1:2	0.161	0.31	4.3
2	0.201	0.97	2:5	0.153	0.47	1.9
3	0.094	0.97	1:2	0.090	0.47	2.2
4	0.133	0.22				6.3
5	0.399	0.99	1:2	0.372	0.46	2.4
6	0.330	0.92	1:2	0.234	0.33	4.3
7	0.088	0.28				n.a.
8	0.304*	0.7*	1:4	0.347	0.4	n.a.
9	n.a.	n.a.	1:2	0.134	0.97	n.a.
10	0.196	0.97	1:2	0.175	0.42	1.9
11	0.157	0.49			0.49	2.9
12	0.100	0.96	1:4	0.136	0.34	4

Table 3: Morphological properties of full-scale samples

Sample	D_{eq} (μm)	L_f (μm)	Nb_f	%Floc	D_f
1	56	1070	17	93	1.34
2	44	1028	17	88	1.34
3	52	780	11	93	1.32
4	61	446	3	82	1.28
5	35	5900	75	52	1.44
6	39	3283	50	72	1.39
7	43	2178	34	83	1.37
8	62	230	8	71	1.44
9	37	623	38	76	1.48
10	44	1490	24	84	1.36
11	46	1593	26	85	1.38
12	40	1350	22	79	1.39

In spite of this problem it appears that the samples which have large flocs have a limited number of filaments per image (Figure 4). The fractal dimension is related to the roughness of flocs: it increases with the total length of filaments (Figure 5a) but decreases when the equivalent diameter increases (Figure 5b). The data points corresponding to samples 8 and 9 could not be taken into consideration because the fractal dimension is very sensitive to the spatial resolution.

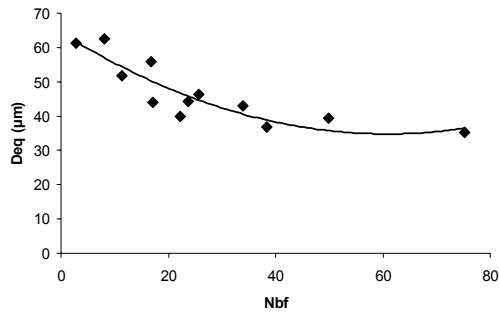
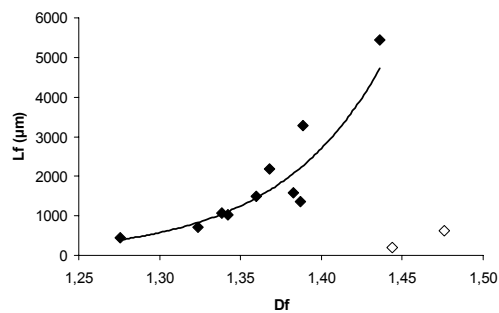


Fig. 4. Variation of the floc equivalent diameter with the average number of filaments / image

a



b

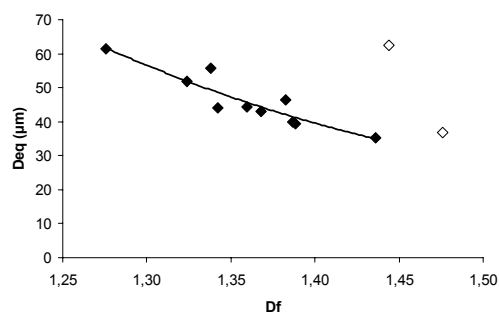


Fig. 5. Relations between the flocs fractal dimension and the total length of filaments / image (a) and the flocs equivalent diameter (b). Samples 8 and 9 are noted (\diamond)

It is difficult to find a general correlation between the *SVI* and the morphological characteristics, especially when *SVI* has to be determined after dilution (Figure 6). The general trend of increase of *SVI* with the abundance of filamentous bacteria mentioned in literature (Richard, et al., 1984) is found but the data are largely dispersed. No relation was found between *SVI* and the flocs fractal dimension.

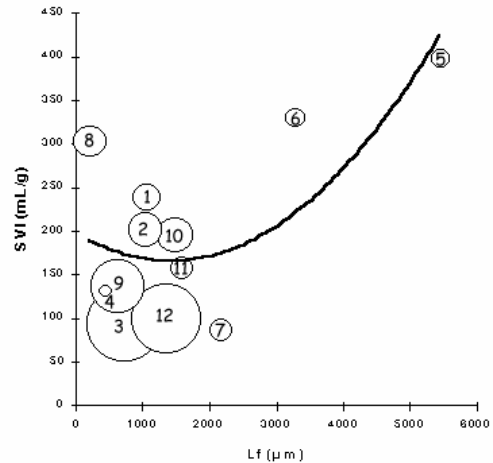


Fig. 6. Relation between *SVI* and the total length of filaments /image. The circle size is proportional to the suspended solid concentration. The data correspond to *SVI* after dilution except for samples 4, 7 and 11

3.3. Macro-scale morphology

Table 4 compare the size measurements at the meso and macro scales: the macro-scale equivalent diameter is always larger by 10 to 20 μm than the meso-scale equivalent diameter, but D_h is very similar to $D_{eq\ meso}$ except for very concentrated filament-rich activated sludge such as the one observed in sample 12.

Table 4: Effect of visualisation magnification on flocs size

Sample	$D_{eq\ meso}$ (μm)	$D_{eq\ macro}$ (μm)	D_h (μm)
1	56	71	56
2	44	60	54
3	52	68	52
4	61	76	58
10	44	54	48
11	46	56	42
12	40	60	110

The fractal dimension at the macro-scale, which increases when the equivalent diameter decreases as at the meso-scale, is larger than the one observed at meso-scale (Figure 7).

IV. CONCLUSIONS

Methods of characterisation of activated sludge in terms of the flocs morphology and the abundance of filamentous bacteria using automated image analysis have been tested on samples from full-scale plants of different designs and operating conditions.

The visualisation is done on fresh samples, which requires a very limited preparation by the operator.

This simplicity limits the visualisation of filamentous bacteria to those outside the flocs. Those forming the backbone of flocs cannot be seen.

At meso-scale, relations could be found between the the abundance of filamentous bacteria evaluated by their total length / image and the floc equivalent diameter in surface on one hand, and the floc fractal dimension on the other hand. The observation at macro-scale brings some complementary information, but which does not seem of major importance for the characterisation of the activated sludge. A single series of images at a magnification of x100, with a good spatial resolution, is sufficient.

The present data, obtained by automated evaluation of filamentous bacteria abundance, confirm the general trend of their variation with *SVI*. Similar results were obtained by da Motta et al. (2000b) on pilot scale experiments with a biodegradable soluble substrate. However a precise relationship seems difficult to obtain, as the flocs equivalent diameter and the suspended solid concentration might play a role. More data, covering larger ranges of these variables, should be considered.

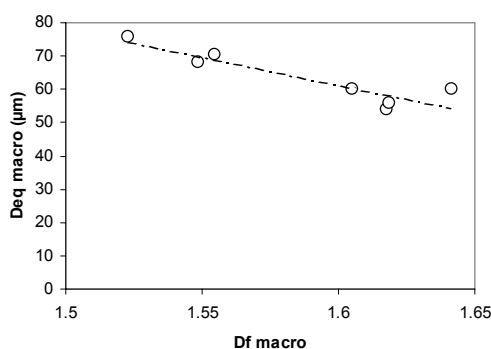


Fig. 7: Variation of D_{eq} versus the fractal dimension at macro-scale

ACKNOWLEDGEMENTS

The authors are thankful to CNPq (Brazil), to the cooperation program of Embassy of France in Portugal and ICCTI, to the city mayors and plant managers.

REFERENCES

Alves, M., A.J. Cavaleiro, E.C. Ferreira, A.L. Amaral, M. Mota, M. da Mota, H. Vivier and M.N.Pons (2000) Characterisation by image analysis of anaerobic sludge under shock conditions, *Wat. Sci. Technol.*, **41**:12, 207-214.

Eikelboom, D.H., A. Andreadakis and Andreasen K. (1998) Survey of filamentous populations in nutrient removal plants in four European countries, *Wat. Sci. Technol.*, **37**, 281-289.

Grijpspeerd, K. and W. Verstraete (1997) Image analysis to estimate the settleability and concentration of activated sludge, *Wat. Res.*, **31**, 1126, 1134.

Kynch, G.J. (1952) A theory of sedimentation, *Trans. Faraday Soc.*, **48**, 621-629.

da Motta M., M.N. Pons, N. Roche, A.L. Amaral, E.C. Ferreira and M. Mota (1999) Analyse des flocs bactériens et de la microfaune des boues activées par analyse d'image, Proc. 3rd Intern. Research Conf. On Water Reuse, Toulouse, 321-326.

da Motta M., M.N. Pons, N. Roche, A.L. Amaral, E.C. Ferreira, M. Alves, M. Mota M. and H. Vivier (2000a) Automated monitoring of activated sludge using image analysis, Proc. 1st World Congress IWA, Paris.

da Motta M., M.N. Pons M.N and N. Roche (2000b) Automated monitoring of activated sludge in a pilot-plant using image analysis, Proc. Watermatex 2000, Ghent.

Richard, M.G. et al. (1984) The growth physiology of the filamentous organisms Type 021N and its significance to activated sludge bulking *57th Ann. Water Pollut. Control Fed. Conf.*, New Orleans.

Richard M. (1991) *Activated sludge microbiology*, The Water Pollution Control Federation, 2nd ed., Virginia, USA.

Russ J.C. (1995) *The image processing handbook*, 2nd ed., CRC Press, Boca Raton.